Voltage Stress in a Transformer Winding During Very Fast Transients Caused by Breaker Closing Event

Tarik Abdulahovic and Torbjörn Thiringer

***Abstract*—Transformers connected at the medium-voltage level in cable grids, such as wind park collection grids and industrial grids, are exposed to the stress of very fast transients. These electric transients are mainly generated during breaker switching operations and the rise time of the transient voltage in such systems is much shorter compared to the rise times of transients generated in transmission systems at a high-voltage level. In this paper, the internal voltage stress is studied during very fast transients generated during transformer energization. Instead of using a breaker, the energizing tests are performed using a low-impedance pulse generator that can generate lightning impulse-shaped waveforms and voltage steps with rise times varying between 35 and 500 ns. Experiments show that during very fast transients with a 35-ns rise time and 1-p.u. magnitude, the interturn voltage exceeds the level obtained with a lightning impulse-shaped voltage waveform of 4.4 pu. Furthermore, during a specific switching scenario with delta-connected transformers, where the winding is excited from both ends, the same 1-p.u./35-ns voltage step generates an interturn voltage that exceeds the 1-p.u. level, which is more than 2.5 times higher voltage stress than during a lightning impulse test.**

***Index Terms*—Cables, power system transients, power transformer insulation testing, transformer windings, transient propagation, transient response.**

I. Introduction

THE lightning phenomenon is considered to be the source of the highest and fastest transients, which electric apparatuses in power systems, such as transformers, are exposed to. The generated voltage pulses have a very steep front in the order of microseconds (μs) and can reach a magnitude many times higher than the system's rated voltage. High overvoltages produced by lightning are mitigated by the use of surge arresters that keep the voltage limited within a range that is not harmful to the protected equipment.

However, SF_6 and vacuum interrupters can produce voltages where the rise time is more than 100 times shorter than the lightning impulse. Furthermore, it is reported worldwide that many transformer insulation failures have occurred possibly by switching operations of vacuum circuit breakers (VCBs), even though the transformers have previously passed all of the standard tests and complied to all quality requirements [1]–[4]. This phenomenon is not related only to VCBs since another study showed that SF_6 insulated breakers and disconnectors can also generate such transients [5]. The breakdown in the SF_6 medium can have a rise time between 2–20 ns, where SF_6 interrupters can also generate voltage restrikes and prestrikes during their operation [5]. Studies of the insulation failures of the motors, caused by the switching phenomenon, showed that the surges generated during switching of the air magnetic CBs are very similar to the surges created with vacuum devices [6], [7]. According to one of these studies, the air magnetic CBs generated surges with a magnitude of 4.4 p.u. and a rise time of 0.2 μs, while the vacuum breaker-generated surges have a 4.6-p.u. magnitude but with a longer rise time of 0.6 μs [6].

A 10-year-long study that included the investigation of failures of thousands of transformers conducted by Hartford Steam Boiler earlier concluded that the high-frequency transients are the main cause of the transformer insulation failure [8]. Furthermore, many studies give a description of the phenomenon that can produce high overvoltages internally in transformer windings [9]–[16]. Although some authors claim that the direct proof of the negative impact of the high-frequency transients on the transformer insulation is not yet found [5], the high-frequency internal overvoltages are considered as a likely cause of transformers insulation failures [9]–[14]. Moreover, even though the voltages at the terminals of the transformer, produced by the closing of the breaker, are well within the limits and do not exceed the magnitude of the peak grid voltage, it is reported that some transformer failures occurred even during such energizing transients [1]–[3].

The goal of this paper is to investigate interturn voltages that appear during winding energization of transformers with interleaved winding with a very fast transient voltage. Moreover, energization of transformers with different winding configurations and different insulation types, using a test reactor, is analyzed. The obtained interturn voltages are then compared with the interturn voltages measured during the lightning impulse test at the basic lightning impulse (BIL), which is considered to be the highest and fastest voltage stress by the transformers standards [17]–[21].

II. Impact of the Transformer's Winding Configuration on Very Fast Transients

The transformer energizing transients depend substantially on the winding arrangement of the high-voltage (HV) side windings. For a wye-connected transformer, one end of the windings is connected to the common neutral point which has a floating potential. The neutral is never exposed directly to a voltage step, since the voltage step is already quite damped when it reaches

Manuscript received June 18, 2013; revised October 04, 2013; accepted December 01, 2013. Paper no. TPWRD-00688-2013.

The authors are with Chalmers University of Technology, Gothenburg 41296, Sweden (e-mail: tarik.abdulahovic@chalmers.se; torbjorn.thiringer@chalmers.se).

Color versions of one or more of the figures in this paper are available online at http://ieeexplore.ieee.org.

Digital Object Identifier 10.1109/TPWRD.2013.2294379

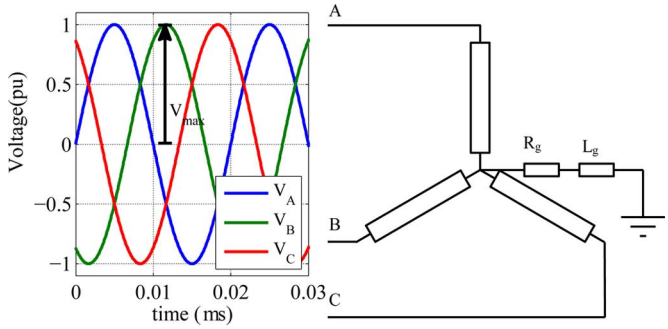

Fig. 1. Voltages at the terminals of the star-connected transformer.

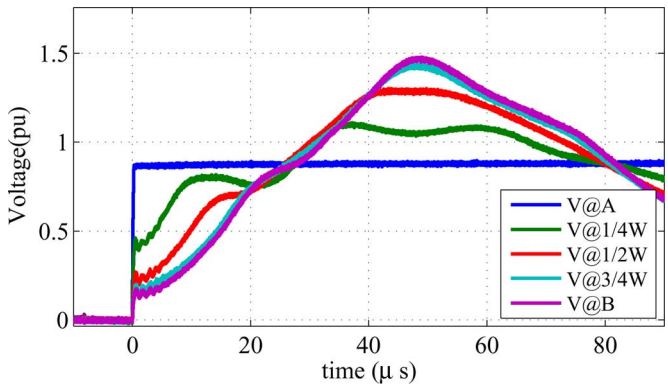

Fig. 2. Measured internal voltages during winding energization.

the neutral point. For a grounded transformer, the neutral point is always at zero voltage if the grounding path is short with a negligible inductance L_g. The maximum voltage that energizes a wye-connected transformer winding during normal operation is the peak phase-to-ground voltage. Transformer terminal voltages and the maximum voltage are presented in Fig. 1.

In medium-voltage (MV) cable grids, the HV transformer side is very often delta connected. This is always the case in wind farms, where the ground connection is done either at the substation transformer or at an auxiliary transformer that is used to supply apparatus. For a delta-connected transformer, a simple energizing transient is a quite complex phenomenon. There are some energizing scenarios that can produce very high internal voltages.

In a delta-connected transformer, the winding is energized from both ends. Moreover, at the moment of energizing of a delta transformer, the voltage at a winding end at the moment of energizing does not necessarily have to be zero like in the case of a wye-connected transformer. Once a delta-connected transformer is energized from a low-impedance source (i.e., cable grid) at one terminal, the energization of the winding's stray capacitance will result in voltage oscillations that oscillate at the winding's resonant frequency since the other ends are open circuited. This is shown in Fig. 2.

The voltage signal is applied from a low-impedance source to terminal A (V@A), while the following lines represent the voltages at one-quarter length, one-half length, and three quarter length of the winding and at the end terminal B (V@B). The initial voltage distribution along the winding is determined by the parallel stray capacitances of the winding. The voltage at the end

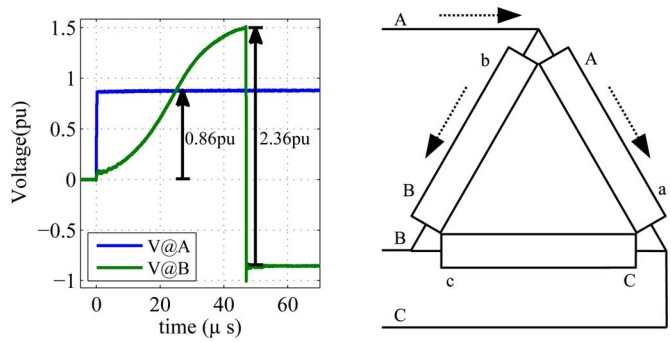

Fig. 3. Delta-connected transformer.

of the winding oscillates with the highest magnitude at the resonance frequency of the winding. In an ideal case, the voltage magnitude at the end of the winding can reach twice the magnitude of the applied step while, in this case, it is about 10% lower, reaching a magnitude of 1.5 p.u. This voltage level is reached after approximately 50 μs or 0.05 ms due to the winding's resonance frequency of about 10 kHz. Due to the voltage oscillations, there is a very likely scenario where the other winding end at terminal B is energized with a negative voltage in a moment when the positive voltage reaches its maximum of 1.5 p.u. Consequently, for a magnitude of the energizing voltage step of -0.86 p.u., it appears as if the winding is energized with 2.36-p.u. voltage. This is the worst case scenario in which the highest voltage step at the end of a delta-connected winding is generated. Such a case scenario is presented in Fig. 3.

Fig. 3 shows the voltage-wave oscillation at the terminal B after the voltage step is applied at the terminal A. In about 48 μs, the voltage wave reaches its maximum at the terminals B and C. If any of these two terminals are energized by a negative voltage step at that moment, the resulting voltage step at that particular terminal will reach 2.36-p.u. magnitude as a result.

The described scenario very likely will not occur during an energizing transient. The initial estimated risk of appearance of such an event is less than 0.5%. However, considering the magnitude of the resulting voltage step, it is worth studying this as a worst case scenario.

III. Test Setup

An experimental setup consists of a reactor, pulse generator, and measurement equipment. The reactor consists of two identical windings rated at 10 kV and 200 kVA when these are connected in series. An aluminum shield is added to the reactor in order to give a more realistic distribution of stray capacitances. Three holes in the front cover are left open in order to provide access to measurement points. The reactor is presented in Fig. 4.

The test voltage steps are generated using a simple electronic circuit, in which a metal–oxide semiconductor field-effect transistor (MOSFET) controlled discharge of a capacitor is utilized. This voltage source has low impedance and its impedance characteristics is similar to cable grids. When the transistor is switched on, the capacitor discharges over the winding. The capacitor is discharged after about 0.5 s, but in a few milliseconds, it appears as a step. This is sufficient enough to consider it as a voltage step, since we are observing transients that are damped

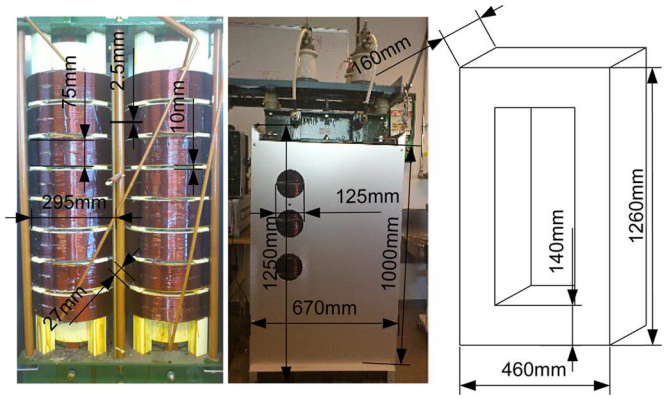

Fig. 4. Test reactor (winding dimensions, shield dimensions, and core dimensions.

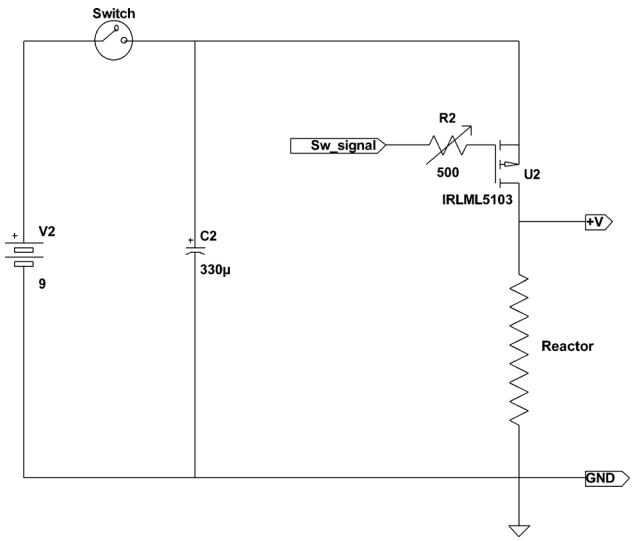

Fig. 5. Pulse generator simplified scheme.

within a few hundreds of microseconds. A 1-m-long coaxial cable is used to transfer the voltage between the generator and the reactor. The rise time is tuned using a variable resistor in the gate circuit of the MOSFET transistor that operates as a switch. The minimum rise time of the voltage step without any load connected to the voltage generator is about 20 ns.

During the tests, two different pulse generators were used. Since the subject of this study is very fast transients, the test voltage level can be in the order of a few volts. This is because the magnetic core for such a short time acts like a magnetic insulation and nonlinear effects of saturation do not exist in that time frame [22]–[24]. Therefore, the voltage level of the pulse generators is between 6 V and 9 V. One generator can make only single pulses and it is used to generate the lightning pulse-shaped voltage waveform. This is done by adjusting variable resistors in the pulse generator that can tune the rise time and the tail time of the voltage waveform. A simplified scheme is given in Fig. 5.

Another pulse generator is used to simulate a case scenario when a delta-connected transformer is energized. In this case, one of the windings of a delta-connected transformer is energized from both ends. One end of the winding is energized by

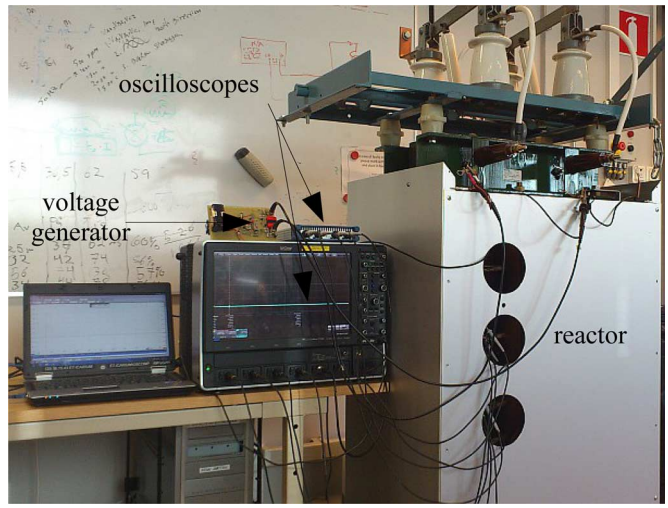

Fig. 6. Measurement setup with reactor.

a positive pulse, while the other one is energized by a negative voltage pulse. The time delay between the positive and the negative pulse can be tuned using a variable resistor. Moreover, in order to estimate the impact of the rise time of a voltage step on interturn voltages, the rise time of both voltage steps can be adjusted as well.

Two oscilloscopes were used simultaneously for the measurements. The same pulse is used to trigger both oscilloscopes and up to seven channels could be measured at the same time. This is because one of the signals is measured at the same time by both oscilloscopes in order eliminate time delays between the trigger times at the two oscilloscopes. The bandwidth of the slower oscilloscope is 1.5 GHz while the probes have a bandwidth of 500 MHz. Measurements were recorded at a sampling speed of 20 MSamples/s and 8-b resolution. During the postprocessing of the data, voltage signals were filtered using a 50-MHz low-pass filter without delay. This is achieved using the *filtfilt* Matlab function. The measurement setup is presented in Fig. 6.

A. Test Reactor

In this paper, one winding of a single-phase 10-kV, 200-kVA reactor is used as a test object. Ideally, in the tests, a three-phase delta-connected transformer would be used, but for the transient studies of a transformer winding, this test reactor is a very good test object.

Each winding of the reactor consists of eight conventional disks. None of the disks have additional voltage reduction measures, such as interleaving. Each disk is wound in the same way, where odd disks are wound starting from the outer layers while even disks are wound starting from the inner layers. Each layer consists of 30 conductors, while each disk consists of 9 layers. The structure of the reactor winding is presented in Fig. 7.

Terminals A and B represent the end terminals of the winding, while disks 4–6 are omitted from Fig. 7.

IV. Analysis of Interturn Voltages

For interturn voltage analysis, the voltage signal generator is used to apply different voltage signals to the reactor's winding. Interturn voltages are analyzed for three different types of

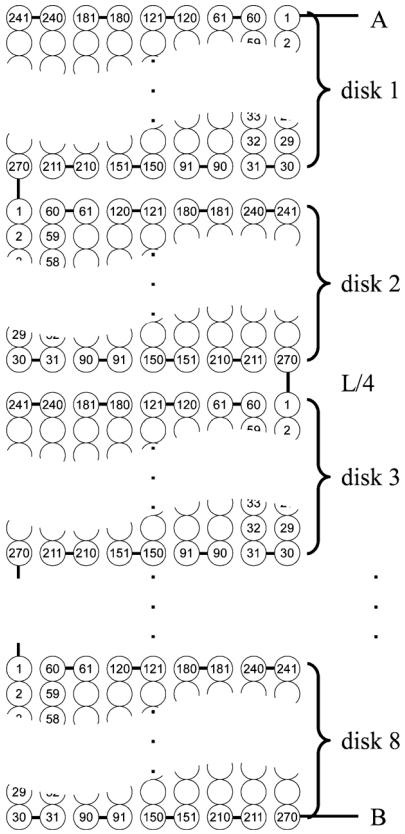

Fig. 7. Reactor winding scheme.

TABLE I
NOMINAL SYSTEM VOLTAGE AND BASIC LIGHTNING IMPULSE INSULATION LEVELS (BIL) FOR DRY-TYPE TRANSFORMERS [17]

	BIL (kV)	45	60	75	95	110	125	150	200
U_{nom}									
8.7		S	1		1				
15			S		1	1			
24					2	S	1	1	
34.5							2	S	1

voltage signals, the lightning impulse, voltage step, and double voltage step, where a negative voltage step is applied to the opposite winding end after a certain time delay. The rise time of the voltage steps is adjusted between 35 and 500 ns.

A. Critical Voltage Stress

The standards for dry-type and oil insulated transformers define the BIL for each voltage level. In order to comply with the standards, tested transformers should not show any sign of insulation damage after the standard tests. These voltage impulse tests are considered as the highest and fastest voltage stress that can impact transformers insulation. It is considered that if a transformer is able to withstand such a voltage stress without any damage, its insulation should survive other high-frequency transients as well. For that reason, the interturn voltage obtained during the lightning impulse-shaped voltage stress is taken as a reference.

The BIL defined by standards for dry-type and oil-impregnated transformers is given in Table I.

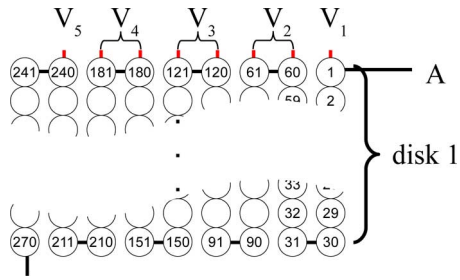

Fig. 8. First disk measurement points.

S is referred to as the standard value, 1 as an optional higher level for high overvoltages, and 2 is an optional lower level when surge arresters are used to limit the voltage level.

These data are used as a reference voltage stress and they are compared with the voltage stress generated with very fast transients. The data are presented in per unit (p.u.) due to the use of low test voltages. The per-unit values are calculated as the ratio of the BIL and the peak phase voltage. For example, for a voltage level of 8.7 kV, the basic lightning insulation level is 6.33 p.u., while for a 34.5-kV voltage level, the BIL value with surge arrester protection is 4.44 and 5.33 p.u. per standard BIL. As the BIL reference, a 4.44-p.u. BIL is chosen since it has the lowest magnitude in per unit and that a 30–40 kV voltage level is used in large offshore wind farms where transformers are usually protected by surge arresters.

B. Interturn Voltages in the 1st Disk

The voltage derivative and the rise time of the voltage step applied to the terminal of the winding decrease significantly along the winding as the wave travels from one terminal to another. Consequently, for very fast transients, the highest interturn voltage is recorded in the beginning of a winding, or in the first disk. Because of this, transformer manufacturers usually apply interleaving in order to decrease the interturn voltage in the top disk. However, such a technique is not used in distribution dry-type transformers.

1) Interturn Voltages During BIL: As mentioned before, the voltages are measured at the top of the disk, and the interturn voltages are calculated. By measuring at the top of a disk, the highest interturn voltages are captured. Fig. 8 shows the measurement points at turns 1, 60(61), 120(121), 180(181), and 240(241), respectively. Although the voltage is measured at only one of the adjacent turns, for example, on turn 60 or turn 61, the voltage difference between these turns is negligible. Therefore, the interturn voltage between turns 1 and 60 is almost identical to the interturn voltage between turns 1 and 61.

In the first test, a low-voltage 1.2/50-μs impulse is applied at the first turn using a low-impedance voltage source. A 4.44-p.u. voltage level is set as a reference since it corresponds to the maximum BIL of a surge arrester protected by the dry-type transformer at a 34.5-kV voltage level. The difference between this test and a real lightning impulse test is that the other end of the winding is left open and not grounded. However, this does not

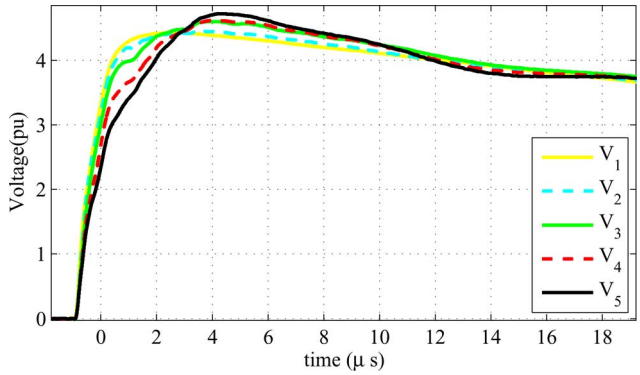

Fig. 9. Turn voltages at the first disk during BIL.

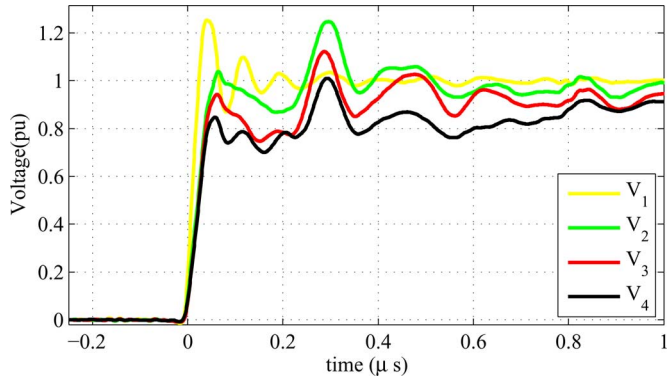

Fig. 11. Turn voltages at the first disk during 35 ns $t_{\rm rise}$ voltage step.

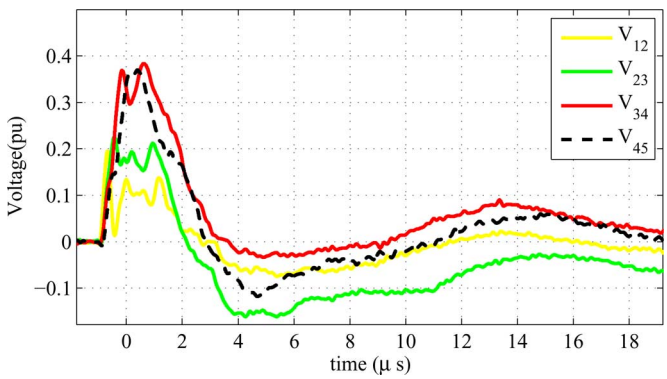

Fig. 10. Interturn voltages at the first disk during BIL.

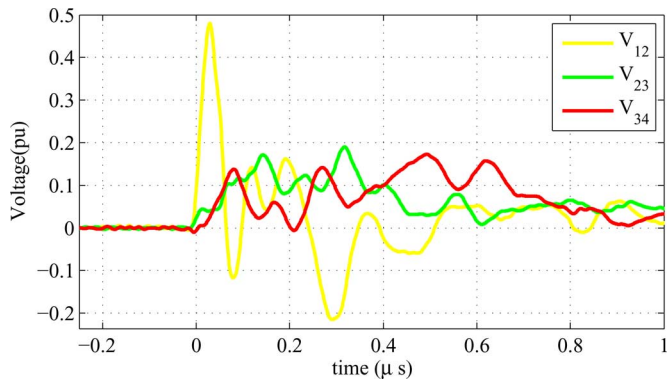

Fig. 12. Interturn voltages at the first disk during 35 ns $t_{\rm rise}$ voltage step.

significantly impact the interturn voltages since the highest interturn voltage is recorded during the rise time of the lightning pulse, during which the voltage at the end disk is almost zero.

Fig. 9 shows the voltages measured at the top turns of the measurement points 1, 2, 3, 4, and 5, respectively. A decrease of the rise time of the propagating voltage is noticed as the pulse propagates through the disk. The magnitude of the voltage increases due to voltage oscillations, and reaches a level of 4.72 p.u.

The plot with interturn voltages is presented in Fig. 10. The interturn voltages V_{12}, V_{23}, V_{34}, and V_{45} show the voltages between adjacent turns 1–60, 61–120, 121–180, and 181–240. It can be noticed that the highest interturn voltage is not developed in the beginning of the disk. Instead, the highest voltage of 0.4 p.u. is obtained toward the second half of the disk. This is the highest interturn voltage stress that appears during the lightning impulse test and it is considered as a reference.

2) Interturn Voltages During Connection of a Wye-Connected Transformer: In order to observe interturn voltages during the connection of a wye-connected transformer, a single voltage step is applied to the reactor winding. This is because that with a wye-connected transformer, one end of the winding is connected to the neutral. The magnitude of the voltage step is set to 1 p.u., which is the peak value of the phase-to-ground voltage. This test is performed with different rise times of voltage steps. This is done in order to account for different transformers insulation types and sizes. It is known that different insulation types make a substantial impact on transformers stray capacitances and, consequently, the rise time of the energizing voltage rise times [25], [26]. For that reason, the rise time is varied between 35 and 500 ns.

Fig. 11 shows the voltages measured at the measurement points 1–5, at the first disk, respectively. Due to a very short rise time of 35 ns, internal interlayer resonances are excited. Furthermore, due to the stray capacitances and inductances between the capacitor that is discharged and the measurement point 1, a voltage ringing appears. This increases the peak voltage to about 1.2 p.u. at the first layer.

The initial frequency recorded at the top conductors at each coil varies between 13.7 MHz in the beginning of the disk, down to 11.5 MHz measured toward the end of the disk. The frequency decreases due to the structure differences. The internal layers are surrounded by neighboring layers, while the outer layer has air as a boundary at one side. As a result, the rise time on the first conductor of the outer layer is two times shorter compared to the rise times recorded on the internal layers. Consequently, the interturn voltage between the outer and the first internal layer is much higher compared to other interturn voltages, which is shown in Fig. 12.

The interturn voltage V_{12} reaches a magnitude of about 0.49 p.u., while the other interturn voltages are substantially lower, with a peak of about 0.2 p.u. The interturn voltage recorded during energization of a wye-connected transformer exceeds the reference interturn voltage of 0.4 p.u. obtained during the BIL test. The peak voltage obtained during such a fast transient is recorded at the beginning of the disk, while during the BIL test, the highest recorded interturn voltage is recorded at the second

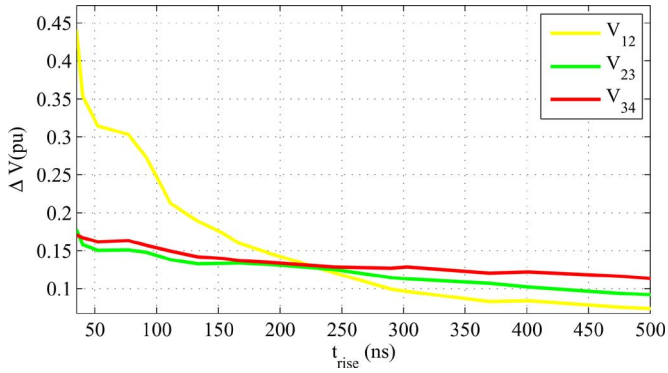

Fig. 13. Interturn voltages at the first disk for different rise times t_{rise}.

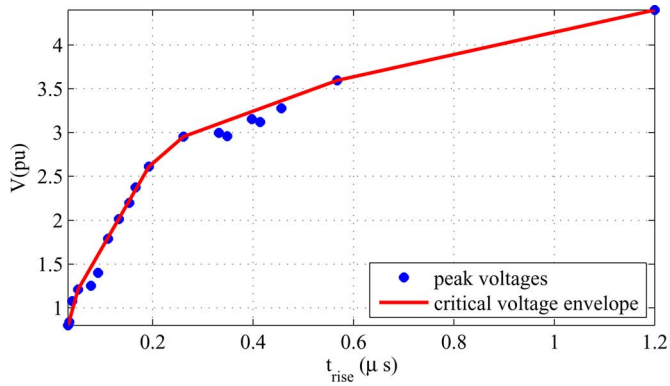

Fig. 14. Magnitude of the voltage transient that generates a maximum-allowed interturn voltage as a function of the voltage transient's rise time.

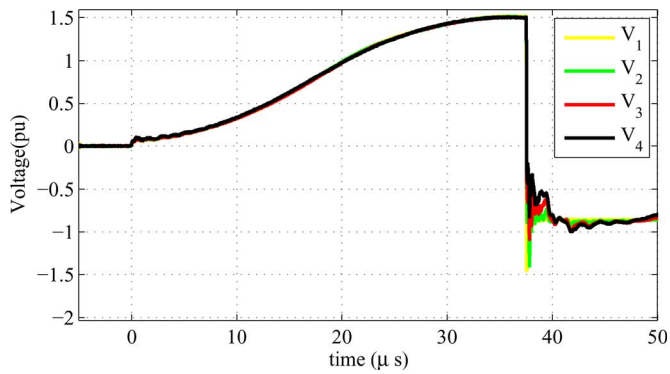

Fig. 15. Turn voltages at the first disk during 35 ns t_{rise} positive and negative voltage step.

half of the disk. This difference appears due to different phenomena responsible for the development of the interturn voltages. In the case of the BIL test, the interturn voltages appear due to internal resonance of the disk, while for very fast transients, a very short rise time of the voltage step yields such a high magnitude of the interturn voltage. Consequently, by increasing the rise time of very fast transients, the interturn voltage drops.

The energization tests are performed for a wide range of rise times. The slowest voltage step have a rise time of about 500 ns. This is done in order to observe the interturn voltages for transformers of different sizes and insulation types. In each test, the rise time is increased by 50 ns incrementally. Fig. 13 shows the interturn voltages at the first disk as a function of rise time.

In Fig. 13, it is observed that there is a quite strong impact of the rise time on interturn voltages. However, for the tested winding, this impact is substantial for voltage steps with rise times shorter than 100 ns. At about 220 ns, the interturn voltages are equal across the entire disk. This is a critical rise time at which the impact of a rise time and a disk resonance on interturn voltages is about the same. With longer rise times, the highest interturn voltage appears toward the end of the disk due to the disk resonance.

The results presented in Fig. 13 are utilized to find out a critical voltage for a given rise time of a voltage step. In other words, these results are used to calculate the magnitude of a voltage step at a given rise time that yields a 0.4-p.u. interturn voltage, which is considered as the highest interturn voltage that a 34.5-kV transformer protected with a surge arrester is designed to withstand. The critical voltage as a function of rise time is presented in Fig. 14.

Fig. 14 shows that the critical voltage decreases substantially when the rise time decreases. For example, a 1.8-p.u./100-ns and a 1-p.u./40-ns voltage step generates an interturn voltage of about the same magnitude as a 4.4-p.u. lightning pulse. It is worth mentioning that the shape of this curve corresponds quite well to the voltage withstand curves of large motors given by the standards [27]–[29]. The direct comparison with the standards is presented in the literature [30], [31].

3) Interturn Voltages During Connection of a Delta-Connected Transformer: For the analysis of interturn voltages during the energization of a delta-connected transformer, two voltage steps are applied simultaneously to both terminals of the winding. The worst case scenario is chosen, where the magnitude of the voltage steps is set to ± 0.86 p.u. This magnitude corresponds to the peak line-to-line voltage $(2 \cdot 0.86 = 1.72 \text{ p.u.} = \sqrt{3} \text{ p.u.})$. However, in order to maximize the voltage stress and achieve the worst case scenario, it is needed to apply the voltage steps with a certain time delay in between, as shown in Section II.

During the tests, the positive step of 0.86 p.u. is applied first at one end of the winding. Consequently, the voltage at the other winding end oscillates at the resonance frequency of the winding, and reaches its maximum after some tens of microseconds. When the maximum is reached, the negative voltage step is applied. This is presented in Figs. 2, 3. and 15.

The test is performed with different rise times of the negative voltage steps in order to study and compare the interturn voltages for different types of insulation and transformers sizes. Similar to the tests with a single voltage step, a 35-ns rise time voltage step is chosen to be the fastest, where a 500-ns rise time is set as a maximum rise time of the voltage pulses.

Fig. 16 shows the zoomed switching transients presented in Fig. 15. Since the negative voltage step is applied at the moment when the voltage reaches about 1.5 p.u., the resulting voltage step has a magnitude of about $1.5 + 0.86$ p.u. $= 2.36$ p.u. Such a fast and HV change generates substantially higher interturn voltages than in the case with a wye-connected transformer.

Fig. 17 presents the interturn voltages recorded at the first disk. As explained before, due to the difference in the physical properties of the outer and the internal layers, where air is a

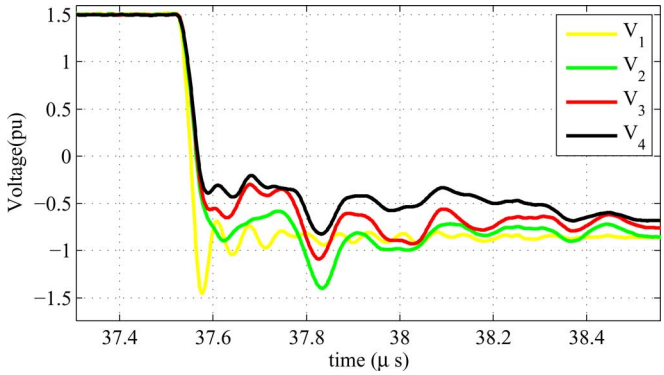

Fig. 16. Turn voltages at the first disk during the 35 ns $t_{\rm rise}$ voltage step.

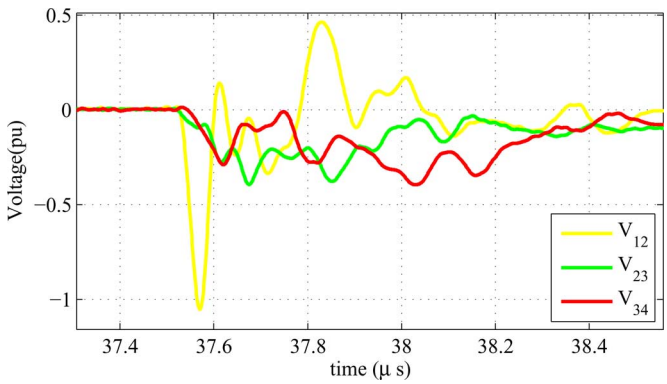

Fig. 17. Interturn voltages at the first disk during the 35-ns $t_{\rm rise}$ voltage step.

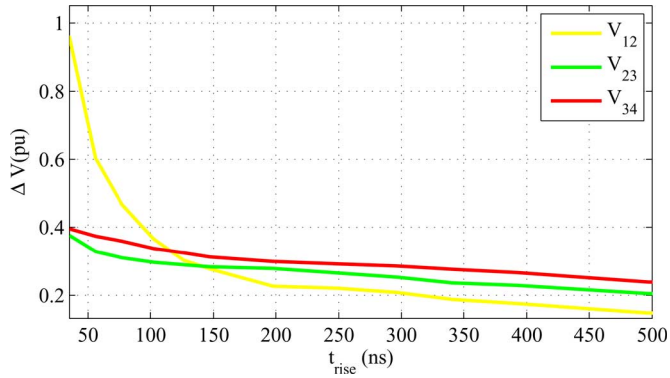

Fig. 18. Interturn voltages at first disk for different rise times $t_{\rm rise}$.

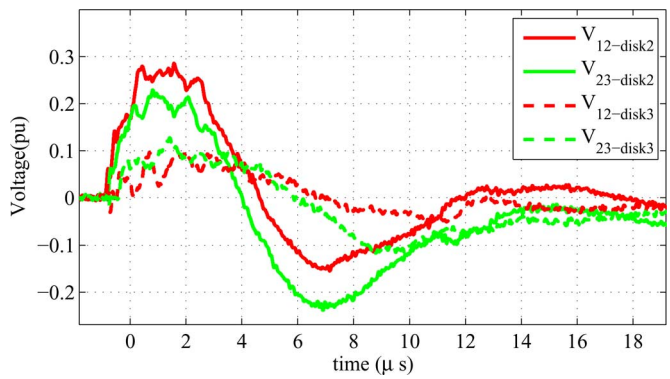

Fig. 19. Interturn voltages due to lightning impulse propagation.

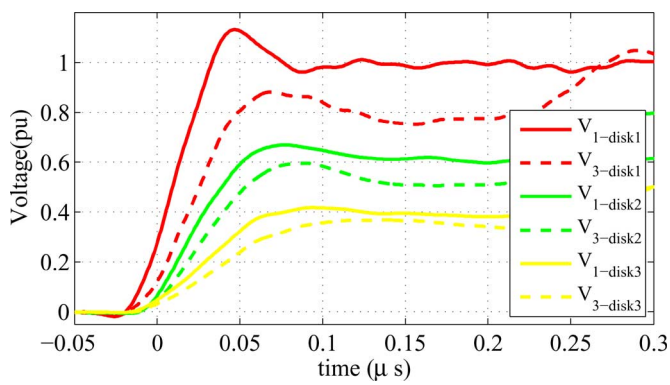

Fig. 20. Wave propagation impact on very fast transients.

boundary of the outer layer, the resonance frequencies of the outer and the internal layers differ substantially. Consequently, the interturn voltage between the first two measurement points V_{12} is much higher compared to other interturn voltages. A maximum interturn voltage of about 1.05 p.u. is reached, which is about 2.5 times higher than the maximum interturn voltage recorded during the lightning impulse test. Furthermore, even V_{23} and V_{34} reach about 0.4 p.u., which is the same magnitude of the interturn voltage as recorded during the lightning impulse test.

In order to obtain the interturn voltage characteristics, more than 10 tests are performed. Fig. 18 shows the interturn voltage curve as a function of rise time. It is worth mentioning that the interturn voltage remains above the critical level of 0.4 p.u. for a broad range of rise times. Only for rise times longer than 95 ns, the interturn voltage drops below the critical level.

C. Interturn Voltages in the Second and Third Disk

After examining the voltage distribution and the interturn voltage stress in the first disk, the $2^{\rm nd}$ and the $3^{\rm rd}$ disk are analyzed. Similar to the measurements on the first disk, the measurement points are selected at the top of the disks, where the highest interturn voltage is expected. The illustration of the measurement points is already presented in Fig. 8.

1) Interturn Voltages During BIL: As shown already before in Fig. 9, the rise time of the voltage impulse and the peak voltage increase as the voltage wave propagates through the disk. Accordingly, the same behavior continues as the wave propagates through the rest of the winding.

Fig. 19 presents the interturn voltages caused by the lightning impulse propagation. As expected, the interturn voltages generated by a lightning impulse decrease along the winding. Compared to the first disk, the magnitude drops in the second disk by 25% to about 0.3 p.u. In the third disk, a magnitude of about 0.1 p.u. is recorded.

When energized by a lightning impulse, oscillations due to resonances appear along the winding.

2) Interturn Voltages During Connection of a Wye-Connected Transformer: The voltage propagation of a 35-ns voltage step is shown in Fig. 20.

Quite a substantial decrease of the voltage derivative and magnitude of the propagating voltage wave is observed. Already in the second disk, the interturn voltages drop by about 40% in magnitude.

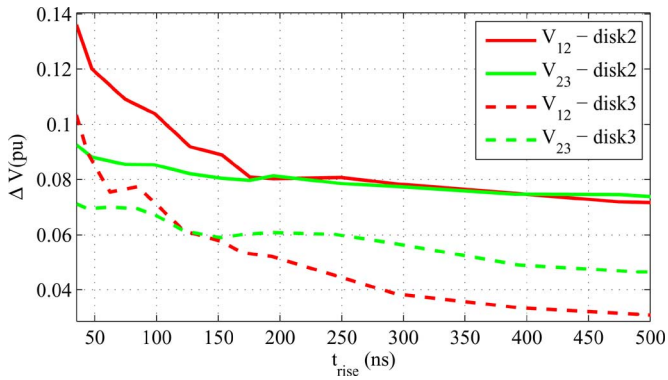

Fig. 21. Interturn voltage in disks 2 and 3 during the energization of a wye-connected transformer.

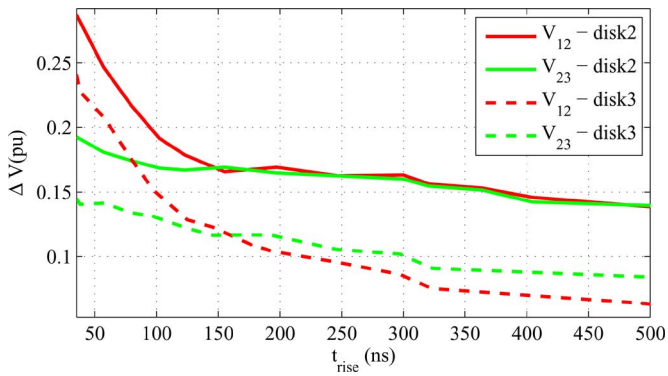

Fig. 22. Interturn voltage in disks 2 and 3 during energization of a wye-connected transformer.

Such a substantial difference between propagation of a lightning impulse and very fast transients is due to the voltage rise time. Very fast transients energize parallel stray capacitances of the winding. This wave follows the path of the stray capacitances and not wires. That is why all of the capacitances are charged within the same time frame, and the voltage is divided accordingly. This is not noted when the winding is energized with a lightning impulse, since it is, in this case, about 35 times slower.

Fig. 21 shows interturn voltages in disks 2 and 3 as a function of rise time. Similarly to disk 1, interturn voltages drop quickly with an increase of rise times. However, the magnitude of the interturn voltages is quite low. In the second disk, it is almost three times lower than the critical voltage of 0.4 p.u., while it is about 4 times lower in the third disk.

3) Interturn Voltages During Connection of a Delta-Connected Transformer: Fig. 22 presents interturn voltages in disks 2 and 3 during the worst case of energizing a delta-connected transformer as a function of rise time. Due to a substantially higher magnitude of the voltage step when a delta-connected transformer is energized, recorded interturn voltages are more than two times higher than in the case of a wye-connected transformer. It reaches the level of the interturn voltage measured during the lightning impulse test. However, the magnitude is still lower than the critical level recorded in the first disk.

V. Conclusion

Voltage tests showed that very fast transients at a rated voltage level can generate interturn voltages which exceed the BIL of dry-type transformers protected with a surge arrester.

In the case of a wye-connected transformer, the critical level is exceeded in the beginning of the first disk for surges with rise times shorter than 40 ns. This means that the standard BIL of 150 kV, or 5.33 p.u., for a wye-connected dry-type 34.5-kV transformer provides a sufficient critical voltage level.

However, very fast transients can generate very high interturn voltages during energization of a delta-connected transformer for rise times shorter than 100 ns. The interturn voltage in the winding used in the tests was 2.5 times higher than the critical voltage recorded during the lightning impulse test for rise times shorter than 40 ns. Furthermore, such a high interturn voltage can appear in the beginning of the first or the end of the last disk.

In order to account for the possibility having such a high interturn voltage stress of delta-connected transformers, the BIL needs to be increased as well. Neglecting the influence of frequency of the interturn voltages on the insulation stress, one can say that the BIL of the delta-connected dry-type 34.5-kV distribution transformers needs to be increased 250% in order to account for this scenario. This even exceeds the optional higher level given by the standards [17] for about 55%.

Acknowledgment

The financial support provided by Vindforsk is gratefully acknowledged.

References

[1] D. D. Shipp, T. J. Dionise, V. Lorch, and B. G. MacFarlane, "Transformer failure due to circuit breaker induced switching transients," presented at the Ind. Comm. Power Syst. Technical Conf., Baltimore, MD, USA, 2011.

[2] D. J. Clare, "Failures of encapsulated transformers for converter winders at Oryx mine," *Electron Mag.*, pp. 24–27, Mar. 1991.

[3] D. Paul, "Failure analysis of dry-type power transformer," *IEEE Trans. Ind. Appl.*, vol. 37, no. 3, pp. 689–695, May/Jun. 2001.

[4] M. Olsen, "Failure analysis of siemens geafol cast-resin transformer," Danish Tech. Inst., Tech. rep. 1154834-1, May 2003.

[5] CIGRE Working Group A2-A3-B3.21, "Electrical environment of transformers—impact of fast transients," *Electra*, no. 208, Feb. 2005.

[6] B. K. Gupta, N. E. Nilsson, and D. K. Sharma, "Protection of motors against high voltage switching surges," *IEEE Trans. Energy Convers.*, vol. 7, no. 1, pp. 139–147, Mar. 1992.

[7] B. K. Gupta, B. A. Lloyd, G. C. Stone, S. R. Campbell, D. K. Sharma, and N. E. Nilsson, "Turn insulation capability of large AC motors—I: Surge monitoring," *IEEE Trans. Energy Convers.*, vol. EC-2, no. 4, pp. 658–665, Dec. 1987.

[8] W. H. Bartley, "An international analysis of transformer failures, part 2—Causes, prevention and maximum service life," *Locomotive*, 1997.

[9] A. Mazur, I. Kerszenbaum, and J. Frank, "Maximum insulation stresses under transient voltages in the HV barrel-type winding of distribution and power transformers," *IEEE Trans. Ind. Appl.*, vol. 24, no. 3, pp. 427–433, May/Jun. 1988.

[10] Y. Shibuya, S. Fujita, and T. Shimomura, "Effects of very fast transient overvoltages on transformer," in *Proc. Inst. Elect. Eng., Gen., Transm. Distrib.*, 1999, vol. 146, no. 5, pp. 459–464.

[11] S. Fujita, N. Hosokawa, and Y. Shibuya, "Experimental investigation of high frequency voltage oscillation in transformer windings," *IEEE Trans. Power Del.*, vol. 13, no. 4, pp. 1201–1207, Oct. 1998.

[12] A. O. Soysal, "Method for wide frequency range modeling of power transformers and rotating machines," *IEEE Trans. Power Del.*, vol. 8, no. 4, pp. 1802–1810, Oct. 1993.
[13] G. Lupo', C. Petrarca, M. Vitelli, and V. Tucci, "Multiconductor transmission line analysis of steep-front surges in machine windings," *IEEE Trans. Dielectr. Elect. Insul.*, vol. 9, no. 3, pp. 467–478, Jun. 2002.
[14] J. L. Guardado, V. Carrillo, and K. J. Cornick, "Calculation of interturn voltages in machine windings during switching transients measured on terminals," *IEEE Trans. Energy Convers.*, vol. 10, no. 1, pp. 87–94, Mar. 1995.
[15] M. Popov, L. van der Sluis, and R. Smeets, "Evaluation of surge-transferred overvoltages in distribution transformers," *Elect. Power Syst. Res.*, vol. 78, no. 3, pp. 441–449, 2008.
[16] M. Popov, R. Smeets, L. Van der Sluis, H. De Herdt, and J. Declercq, "Experimental and theoretical analysis of vacuum circuit breaker prestrike effect on a transformer," *IEEE Trans. Power Del.*, vol. 24, no. 3, pp. 1266–1274, Jul. 2009.
[17] *IEEE Standard Test Code for Dry-Type Distribution and Power Transformers*, IEEE Standard C57.12.91-2011 (Rev. IEEE Standard C57.12.91-2001), 13, 2012, pp. 1–94.
[18] *IEEE Standard General Requirements for Dry-Type Distribution and Power Transformers, Including Those With Solid-Cast And/Or Resin Encapsulated Windings*, IEEE Standard C57.12.01-2005 (Rev. IEEE Standard C57.12.01-1998), 2006.
[19] *IEEE Standard Requirements for Liquid-Immersed Distribution Substation Transformers*, IEEE Standard C57.12.36-2007, 7, 2008, pp. c1–29.
[20] *IEEE Standard for General Requirements for Liquid-Immersed Distribution, Power, and Regulating Transformers*, IEEE Standard C57.12.00-2010 (Rev. IEEE Standardd C57.12.00-2006), 2010.
[21] *IEEE Standard Test Code for Liquid-Immersed Distribution, Power, and Regulating Transformers*, IEEE Standard C57.12.90-2010 (Rev. IEEE Standard C57.12.90-2006), 2010.
[22] P. Gómez and F. De León, "Accurate and efficient computation of the inductance matrix of transformer windings for the simulation of very fast transients," *IEEE Trans. Power Del.*, vol. 26, no. 3, pp. 1423–1431, Jul. 2011.
[23] N. Abeywickrama, Y. V. Serdyuk, and S. M. Gubanski, "Effect of core magnetization on frequency response analysis (FRA) of power transformers," *IEEE Trans. Power Del.*, vol. 23, no. 3, pp. 1432–1438, Jul. 2008.
[24] M. Popov, "Switching three-phase distributions transformer with a vacuum circuit breaker—analysis of overvoltages and the protection equipment," Ph.D. dissertation, Faculty Elect. Eng., Delft University of Technology, Delft, the Netherlands, 2002.
[25] J. C. Das Sr., "Surges transferred through transformers," in *Proc. IEEE Annu. Pulp Paper Ind. Tech. Conf.*, 2002, pp. 139–147.
[26] T. Abdulahovic and T. Thiringer, "Comparison of switching surges and basic lightning impulse surges at transformer in MV cable grids," presented at the Nordic Wind Power Conf., Bornholm, Denmark, Oct. 10–11, 2009.
[27] *IEEE Guide for Testing Turn-to-Turn Insulation on Form-Wound Stator Coils for Alternating-Current Rotating Electric Machines*, IEEE Standard 522-1992, 1992.
[28] *National Electrical Manufacturers Association*, NEMA Standard MG1:20, 2006.
[29] *Rotating Electric Machines, Part 15: Impulse Voltage Withstand Levels of Rotating A.C. Machines With Form-Wound Coils*, Geneva: IEC 34-15, 1995.
[30] T. Abdulahovic, "Analysis of high-frequency electrical transients in offshore wind parks," Ph.D. dissertation, Dept. Energy Environ., Div. Elect. Power Eng., Chalmers Univ. Technol., Gothenburg, Sweden, Dec. 2011.
[31] T. Abdulahovic and T. Thiringer, "Transformers internal voltage stress during current interruption for different wind turbine layouts," in *Eur. Power Electron. (EPE) Wind Energy T&D Chapter Seminar*, 2012.

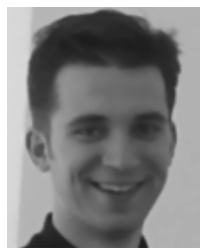

Tarik Abdulahović was born in Srebrenik, Bosnia and Herzegovina, in 1976. He received the Dipl.Ing. degree from University of Tuzla, Bosnia and Herzegovina, in 2001, and the M.Sc. and Ph.D. degrees in electric power engineering from Chalmers University of Technology, Gothenburg, Sweden, in 2006 and 2011, respectively.

Currently, he is with Chalmers University of Technology. His research interests include electromagnetic transients, modelling of electromagnetic transient studies, and electric machines and drives.

Dr. Abdulahović is a member of the CIGRE JWG A2/C4.39 working group on electrical transient interaction between transformers and power systems.

Torbjörn Thiringer received the M.Sc. and Ph.D. degrees in electric power engineering at Chalmers University of Technology, Gothenburg, Sweden, in 1989 and 1996, respectively.

Currently, he is a Professor of Applied Power Electronics with Chalmers University of Technology, His research interests include modelling, control, and grid integration of wind energy converters into power grids as well as power electronics and drives for other types of applications, such as electrified vehicles, buildings, and industrial applications.